

# Use of a Video and Laser System to Quantify Transect Area for Remotely Operated Vehicle (ROV) Rockfish and Abalone Surveys

**Deanna R. Pinkard**  
NOAA NMFS Southwest Fisheries Science Center

**Donna M. Kocak**  
Green Sky Imaging, LLC

**John L. Butler**  
NOAA NMFS Southwest Fisheries Science Center

**Abstract** *In situ* surveys by remotely operated vehicle (ROV) and submersibles are important sampling tools for making fish and invertebrate population estimates. A major challenge associated with these methods is the measurement of the search and/or transect area due to variation in the field of view (FOV) throughout a dive. In addition, to effectively survey complex habitats it is often desirable to adjust the camera angle, which results in significant differences in the FOV in the recorded images and subsequent spatially variant image magnification. This paper describes a method for obtaining accurate surveyed area estimates using FOV measurements derived from image analysis and from the speed of the vehicle measured by a Doppler velocity logger (DVL). The image analysis software considers camera tilt angle, roll and pitch of the ROV, distance from the bottom, and the location of the reference lasers in the imagery to calculate the field of view. The DVL continuously logs forward/aft and port/starboard speeds for a representation of the vehicles movement over the bottom, and in effect, distance traveled. The development of these methods has led to a highly accurate estimate of transect area that will be used to calculate densities of commercially important rockfishes and endangered white abalone in the Southern California Bight.

## I. INTRODUCTION

Many advances have been made since the invention of photographic technology that have enabled scientists to view and record sea life beyond depths that are accessible to scuba divers [1, 2]. The goals of researchers have moved from simply viewing and possibly collecting animals to the desire to know exact locations, depths, search areas, and environmental variables associated with study specimens. The technology has advanced to such a degree that researchers can now use underwater video surveys as part of sound and quantitative ecological survey designs [1, 4, 5, 6]. These advances have allowed for sampling methods that, unlike traditional trawl surveys, are non-destructive and provide additional information including *in situ* observations of habitat characteristics and animal behavior.

Quantifying the actual area searched during video surveys has been a challenge to researchers who need accurate search effort information to estimate density. The complexity of the video system design is the main factor that determines the complexity of the search area calculation. For a sampling design that includes a camera mounted downward in a fixed position moving over the bottom at a nearly uniform height and speed, calculations of field of view (FOV) and distance

traveled are relatively simple because the FOV remains constant.

For more complex survey designs where the camera tilt changes and height above the substrate and speed vary, calculation of the FOV becomes more involved. Systems designed for use under these conditions often include reference lasers and knowledge of altitude and pitch and roll of the camera for precise measurements of the field of view at chosen time intervals [4]. Using this information, the survey area can be calculated using several different methods – all involving time series images (TSI). TSI comprise a plurality of images (still or video in any format, including non-visual images such as infrared, Doppler, etc.) recorded as a sensor platform travels over parallel paths of an observation area (eg. transects).

There are several possible approaches for calculating distance traveled, including simply calculating distances from USBL-provided northing and easting positions, or the use of an accurate Doppler Velocity Logger (DVL) to provide speed information, and in effect a measure of distance traveled. The output from the chosen methods for quantifying distance traveled can be input into quantitative measurement software (QMS™) for a relatively simple calculation of FOV in each image and the total area surveyed. The aim of this study was to design a system to accurately quantify the area surveyed by a remotely operated vehicle (ROV) for the purposes of obtaining rockfish and abalone density per unit area values. These values will ultimately be used for overall population estimates and population monitoring.

## II. MATERIALS AND METHODS

### A. ROV Surveys

All surveys were conducted with a Phantom DS4 ROV. Rockfish surveys took place on board the F/V *Outer Limits* (length = 21 m), and abalone surveys took place on board the R/V *David Starr Jordan* (length = 52 m). The ROV was equipped with the following components (summarized in Table 1): five Class III Diode lasers, an acoustic Doppler current profiler (ADCP)/DVL, pitch and roll sensor, sonar, temperature probe, depth sensor, flux gate compass, digital still camera, and a high definition video camera. WinFrog Integrated Navigation System was used for vehicle navigation and data collection and integration purposes.

*Proceedings of the ITS Oceans 2005 Meeting, August 2005.*

TABLE I  
RELEVANT ROV COMPONENTS

Data Collected	Specifications
<b>ADCP/DVL</b>	
· Forward/aft, port/starboard, and up/down speeds (m/s)	· RD Instruments
· Height off bottom (m)	· 0.4 % speed accuracy
	· 1-4 % altitude accuracy
	· $\pm 0.2$ mm/s velocity drift at zero speed
<b>Digital Still Camera</b>	
· High resolution photos	· Insite Pacific, Inc.
	· Scorpio Plus system
	· Nikon Coolpix 995
	· 3.2 Megapixels
<b>Video Camera</b>	
· Video	· Insite Pacific, Inc.
	· Sony CCD
	· 180° tilt
	· > 450 lines resolution
	· Wide angle glass hemispherical viewport
<b>Lasers</b>	
· Distance measurements	· Class III Diode
· Scale for size estimates	· 2 fixed 60 cm width
	· 2 fixed 13 cm width and 1 angled inward at 83.4°
<b>Pitch and Roll Sensor</b>	
· Position of the vehicle relative to horizontal	· Mounted in line with the camera
· Camera tilt	· Data displayed on an on-screen display

During ROV surveys an attempt was made to pilot the support vessel and the ROV at speeds of < 1 knot in order to effectively survey. This was not always possible due to oceanographic conditions. When speed exceeded 1 knot a note of “off effort” was made for later removal of the data from total area calculations. Abalone surveys included transects near the substrate to search for and photograph all abalone, but specifically white abalone, *Haliotis sorenseni* (see [2] for details). Rockfish surveys were comprised of transects near the substrate and in the water column to survey and photograph individual and schooling rockfish in and over rocky habitats. All tracklines were mapped using ArcGIS ArcMap for a visual representation of the areas surveyed by each transect, including bathymetry and bottom typing information when available. Fig. 1 provides an example ArcGIS map. For this paper, we selected one rockfish ROV dive for processing to compare several area survey quantification techniques.

### B. The Laser Configuration

The primary laser configuration for the video imagery consisted of two fixed, parallel lasers and one crossing laser, as shown in Fig. 2. Assuming a planar substrate, this configuration allowed for computation of range from the camera to the substrate (plane), spatially variant (x,y) scale, center width of the video image, and placement of a known-

sized perspective area graphical overlay in each video frame. Two secondary parallel lasers (not shown in Fig. 2) were centered about the digital still camera located below the video camera. These lasers provided scale information for captured digital still images, along with additional scale and range information when visible in the video imagery.

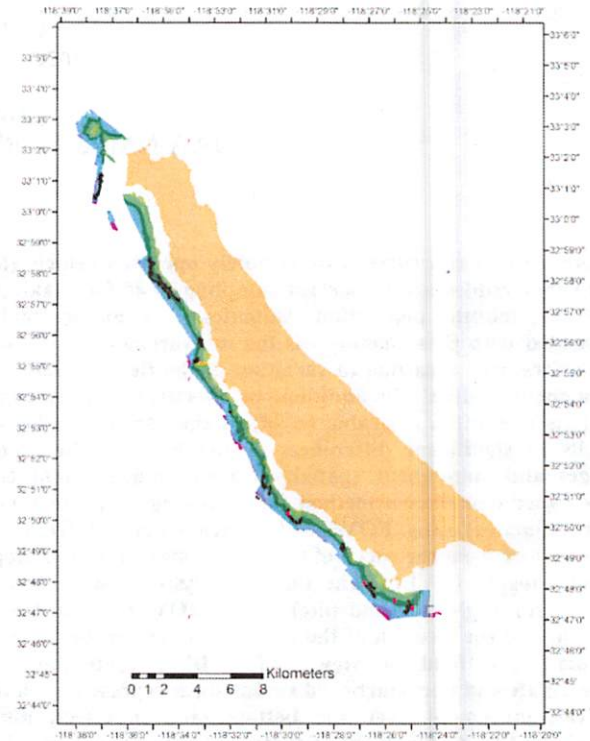


Fig. 1. ROV transect tracklines (black) for an abalone cruise in August 2005. Tracklines are overlaid onto multibeam bottom data. Abalone sightings are represented by red dots.

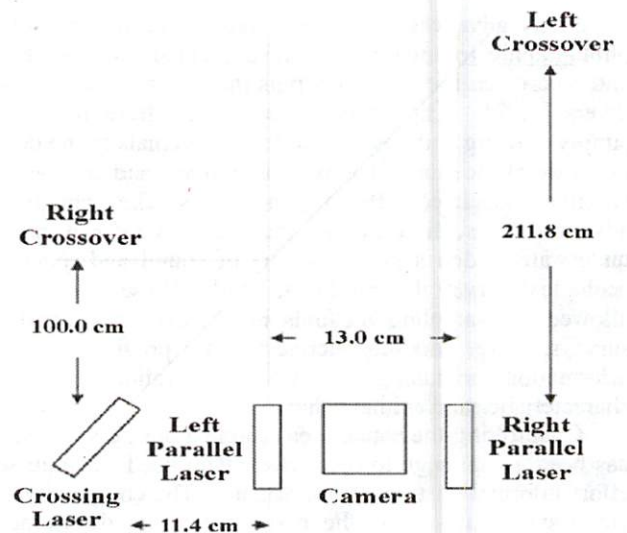


Fig. 2. Laser and camera set up displaying calibrated distances between lasers and crossover points.

### C. Width of the Field of View

Prior to using automated software, center widths of the FOV were computed manually for 10 frames chosen at equal intervals, and then averaged to obtain a value for use over the entire length of the transect. Frames were captured using image analysis software (Image-Pro Plus v. 4.5.1.23), and for each frame the distance between the two parallel lasers was measured. Using the known separation distance of the lasers we calculated the width of the FOV (i.e. viewable screen width).

Using the QMS<sup>TM</sup> software, the center width measurements were automatically obtained in all of the processed images. The software used the vehicle's roll to correct (i.e. remove) the rotational component in each image and used the location of the reference lasers to compute the horizontal scale at the center of the image. From this, the center width was computed just as in the manual computation. An example processed image is shown in Fig. 3. In this figure, the center width of the image was measured along the center line of the perspective area overlay, from the leftmost to the rightmost edge of the image, as denoted by the arrows.

Video was captured in a digital format at 10 frames per second and automatically processed by the software based on a pre-selected interval; for example, every  $n^{\text{th}}$  frame, every  $x$  second, every  $y$  meter, or each *randomly generated* frame. If a laser projection was not automatically localized in an image, the user selected the projections manually and the algorithm proceeded to the next image. The processing rate of the QMS<sup>TM</sup> software was varied to examine the appropriate level of sampling necessary to obtain accurate width estimates. In images where one or more of the lasers were not visible and could not be selected automatically or manually, the center width was initially set to zero (or skipped). This condition typically occurred when an object such as a fish or coral occluded the lasers. If a small number of images were skipped (i.e., up to 3 in a row), the center width was assumed to be equal to that of the preceding width calculation. In cases where there are a large number of skipped images that are confirmed to be active searching, interpolation between the preceding and subsequent data points can be implemented.



Fig. 3. Example of a processed image from QMS<sup>TM</sup> software showing location of lasers, 0.5 m x 0.5 m perspective area overlay, and center width.

### D. Distance Traveled

Distance traveled ( $D_{total}$ ) throughout the entire transect was calculated by several different methods for the sake of comparison. The first method computed the distance traveled ( $d$ ) between each of the  $n$  sample intervals by summing the difference in two adjacent USBL positions (Northings ( $N$ ) and Eastings ( $E$ )), and then calculating  $D_{total}$  as follows:

$$(2.1) \quad d_i = \sqrt{(N_n^2 - N_{n+1}^2) + (E_n^2 - E_{n+1}^2)}$$

$$(2.2) \quad D_{total} = \sum_{i=1}^{n-1} d_i$$

A speed filter was applied to eliminate resultant  $d$  values greater than 2.5 m over a 2 s sample period. When a  $d$  value exceeded 2.5 m, the closest data point  $\leq 2.5$  m was used instead. We chose 2.5 m because 1.25 m/s was the greatest speed measured by the DVL during effective searching.

The second method calculated  $D_{total}$  as follows:

$$D_{total} = \left( \sum_{i=1}^{n-1} \sqrt{FRS_i^2 + PSS_i^2} \right) \times \Delta t \quad (2.3)$$

Here, the forward/reverse ( $FRS$ ) and port/starboard ( $PSS$ ) speeds measured by the DVL were used at every sample. Multiplying this summation by the sample interval ( $\Delta t = 2$  s) yielded the total transect distance.

### E. Area Calculations

A Width Sampling Technique (WST) was used to compute the total survey area ( $A_{WST}$ ) using the following equation:

$$(2.4) \quad A_{WST} = \sum_{i=1}^{n-1} d_i \times w_i$$

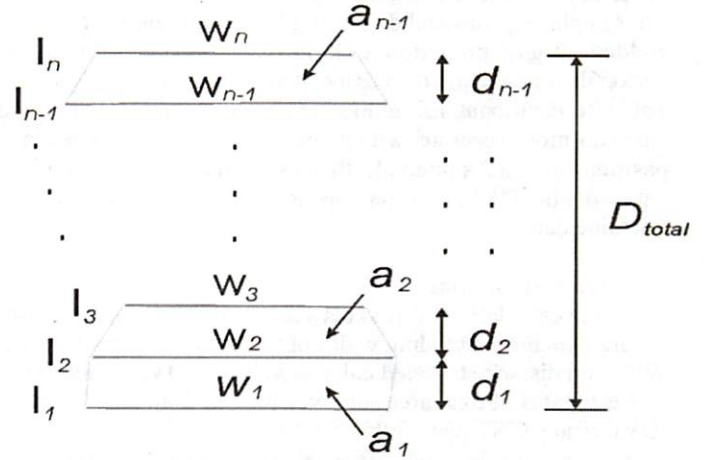


Fig. 4. Diagrammatic representation of the WST used to measure transect survey area.

In this technique (refer to Fig. 4), the center width ( $w_1, w_2, \dots, w_{n-1}$ ) of each image ( $I_1, I_2, \dots, I_{n-1}$ ) is multiplied by the distance traveled from the preceding image ( $d_1, d_2, \dots, d_{n-1}$ ) to obtain an area ( $a_1, a_2, \dots, a_{n-1}$ ). Each of the areas are then summed to obtain a total area ( $A_{WST}$ ) over the entire transect ( $D_{total}$ ).

The area calculations were performed using a combination of the FOV width measurements and the different distance traveled estimates (Northings/Eastings and DVL) to allow for comparisons between methods.

### III. RESULTS

#### A. FOV Width

Using simplified, manual methods to obtain an average center width of the FOV for the sample dive led to an estimate of 2.7 m to be used for the entire dive. The images were sub-sampled by the QMS<sup>TM</sup> software to match the sample rate of the DVL ( $\Delta t = 2$  s), and measured FOV widths ranged from 0.53 m- 5.43 m, with an average width of 1.99 m. For 7 % of the images captured the lasers could not be identified by either the software or manual selection. As mentioned previously, in cases where this occurred in three or fewer sequential images, the previous width estimate was used. In cases (7; total time = 5 min 10 s) when the lasers could not be located in more than three sequential images due to either an “off effort” search status or due to active, “off-bottom” searching (i.e., none of the laser “spots” were visible), the FOV was recorded as 0. One indication of these conditions was a positive or slightly negative ( $> -8.0^\circ$ ) pitch.

#### B. Distance Traveled

The results of distance traveled calculations varied between methods as shown in Table 2. Using Northings and Eastings positions and calculating the change in position every 2 s led to a total track length that was considerably higher ( $> 0.5$  km) than that calculated using the speeds/positions from the DVL. Unrealistic values associated with Northings and Eastings positions were common, and a filter that replaced any distance traveled values that were  $> 5$  m from the previous position with the previous distance traveled value was necessary to remove extraneous positional data. Even with a filter in place, positional data using Northings and Eastings yielded a higher proportion of large distances traveled in a 2 s period than positional data associated with the DVL (Fig. 5; Table 2). Positional information extracted from the DVL speed data was more accurate, with no cases of large differences in positions over a 2 s interval. Because of the consistency of data from the DVL, no filter was used to process the dive trackline data.

#### C. Area Calculations

Area calculations varied between methods, with the most accurate method including width of the FOV calculated by the WST and distance traveled calculated by the DVL (Table 2). The estimates of total area surveyed ranged from 3,053.2 m<sup>2</sup> (DVL  $d$  and WST  $w$ ) to 8,053.5 m<sup>2</sup> (raw N and E  $d$  and average, non-QMS<sup>TM</sup>  $w$ ). Area calculations based on the calculated average width of the FOV were not representative of the true area surveyed because the width of the FOV for this particular dive changed often and dramatically.

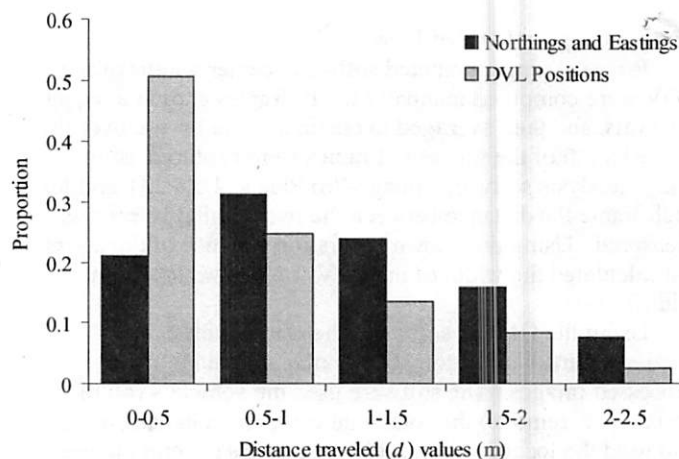


Fig. 5. Distribution of measurements of  $d$  calculated using DVL positions and filtered Northings and Eastings positions.

TABLE II  
DISTANCE TRAVELED AND AREA ESTIMATES FOR A SAMPLE ROV DIVE

Estimate	N's and E's	DVL Positions
Total transect length (m)	<sup>1</sup> 2,982.8 m; <sup>2</sup> 2,430.8 m	1,577.2 m
% $d > 2.5$ m	<sup>1</sup> 8.1 %; <sup>2</sup> 0.0 %	0.0 %
Area - average width of FOV	<sup>1</sup> 8,053.5 m <sup>2</sup> ; <sup>2</sup> 6,563.2 m <sup>2</sup>	4,258.6 m <sup>2</sup>
Area - WST	<sup>1</sup> 5,949.5 m <sup>2</sup> ; <sup>2</sup> 4,809.7 m <sup>2</sup>	3,053.1 m <sup>2</sup>

<sup>1</sup>raw, unfiltered positional data; <sup>2</sup>speed-filtered positional data

### IV. DISCUSSION

The use of ROVs for monitoring of commercially important marine organisms is a non-lethal and cost-effective approach that can yield reliable population estimates for fisheries management. The challenge of obtaining realistic positioning and distance data has been met by the technological advances made in the field of photogrammetric imaging. The system described in this paper is a major improvement of precision over previous methods.

The most reliable estimates of width of the FOV were obtained by the WST method, in which the center width of the FOV was measured at a predetermined rate. Conversely, an average of the manually measured FOV estimates were clearly not representative of the entire transect, as width of the FOV changes frequently. The rate of image capture processing in QMS<sup>TM</sup> (limited only by the camera and/or digitizer specifications) can be altered to satisfy particular sampling needs and to be synchronized with the rate of instrument data collection. In our study, we found that computing the FOV width every 2 s provided a level of accuracy that is acceptable, but not ideal. In the future, we will increase our data collection rate to at least a 1 s interval to allow for more precise measurement and interpolation between data points.

One issue that became apparent while processing the FOV data involved the present inability of the QMS™ software to process video images when the view does not provide a platform for the lasers to project. If the period of time when the lasers are not visible is relatively short (< 10 s), techniques can be applied to fill in the missing FOV data with preceding or subsequent data (see Materials and Methods). When the search strategy includes long periods of time in areas without a bottom (e.g. water column surveys), the issue becomes more difficult to solve. Fortunately, off-bottom searching was rare during the present study (total time was 2 min, 10 s out of the 1 hour, 15 min, 4 s long dive), but for other studies this issue may cause be the cause of sampling limitations. One solution may involve a FOV measurement based solely on the pitch angle during long periods of search time when the bottom is not in view. In addition, FOV could be measured using a known-sized object suspended in the water column for reference.

Although unnecessary for the present study, for some scientific applications it may be desirable to analyze only the center portion of sampled images. Typically in this region lighting is optimized and we can eliminate the effects of edge distortions or aberrations in the lens, providing the best optic conditions for species identification or other optically sensitive processes. In the present study we used a high resolution digital still camera for species identifications, while other researchers may rely solely on video images. In such cases, a perspective area technique (PAT) for computing the survey area can be employed. This method uses only the fixed-size, perspective area centered in each processed image for area calculation (see Fig. 3). Processing is timed to avoid or minimize overlap and gaps between successive images. The sample rate can be determined using an acoustic ranger or broad area optical imager to provide an instantaneous estimation of range at each sample. This eliminates the need to process every image to determine the range using the laser projections. Using this method, the distance traveled is determined using one of the techniques described in Section D and the equation for computing the area is simply:

$$(2.5) A_{PAT} = \sum_{i=1}^n a_i$$

where  $a$  is the user-selected, fixed size in each image ( $i$ ).

Generally, fewer images are required for processing using PAT. However, the advantages of WST derive from rapid sampling of image scale changes with platform motion along the survey track. Instantaneous altitude changes over the substrate are captured at every sample point (i.e., at every image) as the number of pixels in the image varies according to the distance between the camera and the image region. Only ambiguity arising from terrain variations along the track of the platform may cause errors in the calculated area. However, this disadvantage can be ameliorated by recording images at a faster rate.

Distance traveled calculations have been improved simply by the addition of the DVL to measure speed of the vehicle. Speed estimates lend for an accurate measure of the distance the vehicle traveled over any period of time. One limitation of the DVL is the absence of data collection when the ROV is too

close to the substrate (< 0.5 m). At this point the speed data is unreliable, and cannot be used to accurately position the vehicle. Because of this potential constraint the use of DVL data along with USBL positional data may be the solution to provide constant positioning data and, in effect, distance traveled data. Although clearly unreliable on its own, USBL

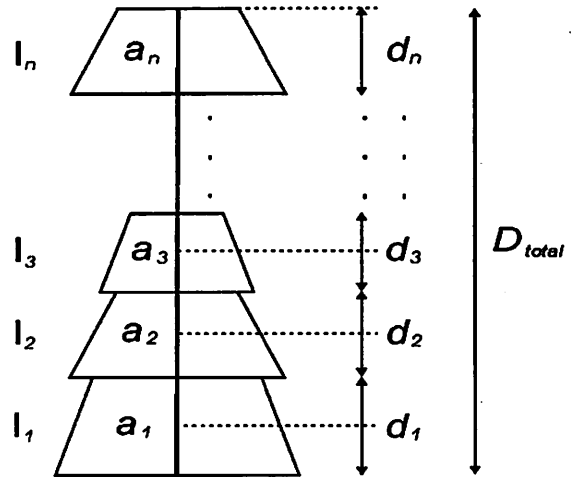


Fig. 4. Diagrammatic representation of the PAT used to measure transect survey area.

data can be useful to fill in the few gaps where the DVL is inaccurate. We plan to explore options for combining these data, including the potential use of filters (e.g. Kalman Filter) and other post-processing possibilities to obtain the most realistic transect tracklines possible.

Area estimates were reliable and at an acceptable level of accuracy when using a combination of the QMS™ WST methods for  $w$  and the DVL data for  $d$ . An issue that did not ultimately halt, but did slow down data processing was time synchronization of all instruments. Although seemingly a simple task, assuring that all instruments are in exact synchronization is an extremely important factor for post-processing. Drift in clocks occurs often and must be adjusted for. The next and final step in our process of improving methods will include further validation of our area estimates by rigorous field testing and calibrations of the DVL and USBL. At this point the system will provide a tool for quantifying area that is extremely precise and reliable for obtaining fisheries population estimates and to monitor populations.

#### ACKNOWLEDGMENT

The authors would like to thank Scott Mau and David Murfin for technical support with the ROV and laser configuration; Mike Wilson for video tape analysis; Carolyn Hall and Lara Asato for participation in the ROV cruises; owner Ken Franke, Captain Paul Fischer, and the crew of the F/V Outer Limits for their assistance with ROV operations; Ben Maurer for his help with manual field of view calculations; and John Kloske for assistance with the distance traveled calculations.

#### REFERENCES

- [1] P. Adams, J. Butler, C. Baxter, T. Laidig, K. Dahlin, and W. Wakefield, "Population estimates of Pacific coast groundfishes from video transects and swept-area trawls", *Fish Bull*, vol.93, pp.446-455, 1995.
- [2] J. Butler, M. Neuman, D. Pinkard, R. Kvitek, and G. Cochrane, "New estimates of habitat and abundance of white abalone (*Haliotis sorenseni*) in southern California", submitted to *Fish Bull*
- [2] J. Butler, W. Wakefield, P. Adams, B. Robison, and C. Baxter, "Application of line transect methods to surveying demersal communities with ROVs and manned submersibles", *Proc. MTS/IEEE*, pp.689-696, 1991.
- [3] D. Kocak, F. Caimi, *Computer vision in ocean engineering*, in *Ocean Engineering Handbook*, F. El-Hawary, Ed. Boca Raton FL, CRC Press, 2001, pp. 4-20.
- [4] D. Kocak, F. Caimi, T. Jagielo, and J. Kloske, "Laser projection photogrammetry and video system for quantification and mensuration", *Proc. MTS/IEEE Oceans*, pp. 1569-1574, 2002.
- [5] B.A.J. Barker, D.L. Davis, and G.P. Smith, "The calibration of laser-referenced underwater camera for quantitative assessment of marine resources", *Proc. MTS/IEEE Oceans*, 3, pp. 1854-1859, 2001.
- [6] D.M. Parry, M.A. Kendall, D.A. Pilgrim, and M.B. Jones, "Identification of patch structures within marine benthic landscapes using remotely operated vehicle", *J Exp Mar Bio and Eco*, pp. 285-286, 497-511, 2003.